



ELSEVIER

1 January 2001

OPTICS
COMMUNICATIONS

Optics Communications 187 (2001) 219–230

www.elsevier.com/locate/optcom

Diode lasers for fast-beam laser experiments

Vladislav Gerginov, Brian Laughman, Diana DiBerardino, Robert J. Rafac,
Steven T. Ruggiero, Carol E. Tanner *

Department of Physics, University of Notre Dame, 225 Nieuwland Science Hall, Notre Dame, IN 46556-5670, USA

Received 18 September 2000; received in revised form 30 October 2000; accepted 6 November 2000

Abstract

This paper describes the diode laser system we use for our fast-beam laser experiments. The air-tight housing, temperature controller, and current controller are described in detail. Data are given for the temperature stability and current noise of the system. A contour map shows the dependence of laser wavelength on temperature and injection current, from which laser frequency scan rates are determined. Fluorescence and absorption spectra of the ^{133}Cs $6s^2S_{1/2} \rightarrow 6p^2P_{1/2}$ and $6p^2P_{3/2}$ resonances are shown for a fast beam, a thermal beam, and a room temperature cell, demonstrating the laser tuning capabilities and spectral width. A radio-frequency sideband technique with a Cs absorption cell is used to demonstrate robust absolute laser frequency stabilization suitable for fast beam applications. © 2001 Elsevier Science B.V. All rights reserved.

PACS: 42.55.-f; 42.55.Px; 42.60.-v; 46.62.Fi; 32.70.Cs

Keywords: Diode laser; Fast-beam laser; Atomic lifetimes; Laser spectroscopy

1. Introduction

This paper describes the design of the diode laser systems that we use for our fast-beam laser experiments [1,2]. Diode lasers are commercially available in a variety of wavelength regions. They are especially suited for our application because of their impressive intensity stability and their relative ease of use. A number of atomic physics experiments employ diode lasers, some of which are discussed in the literature [3]. We have investigated a variety of approaches with the goal of creating a

simple and reliable diode laser system that would be useful for accelerator based experiments where a great deal of attention must be focused on other aspects of the apparatus or where the lasers may be inaccessible during an experimental run. Special efforts are taken to ensure continuous stable operation for many hours. Three main parameters determine the spectral characteristics of diode lasers: temperature, injection current, and optical feedback. The current and temperature are coupled because changes in the current strongly affect the temperature of the diode. For a diode laser to produce a spectrally narrow single-mode output, the injection current must be supplied with a stable direct current (DC) source. To eliminate frequency drift, the diode laser temperature must be electronically stabilized. Each diode laser is tuned by

* Corresponding author. Tel.: +1-219-631-8369; fax: +1-219-631-5952.

E-mail address: carol.e.tanner.1@nd.edu (C.E. Tanner).

selecting an optimal temperature and injection current.

2. Diode lasers

The low lying electronic states of cesium addressed in our atomic lifetime experiments [1] are shown in Fig. 1. The diode lasers we use operate in a free-running mode with a spectral bandwidth of tens of megahertz which is adequate for this application. With the laser crossing the fast cesium beam at a right angle, three effects broaden the resonance. The limited transit time of the atoms through the laser beam produces approximately 100 MHz of homogeneous broadening, the transverse-velocity spread, 0.1 eV, of the 50 KeV Cs beam adds an additional 1 GHz of inhomogeneous broadening, and spontaneous emission adds 5

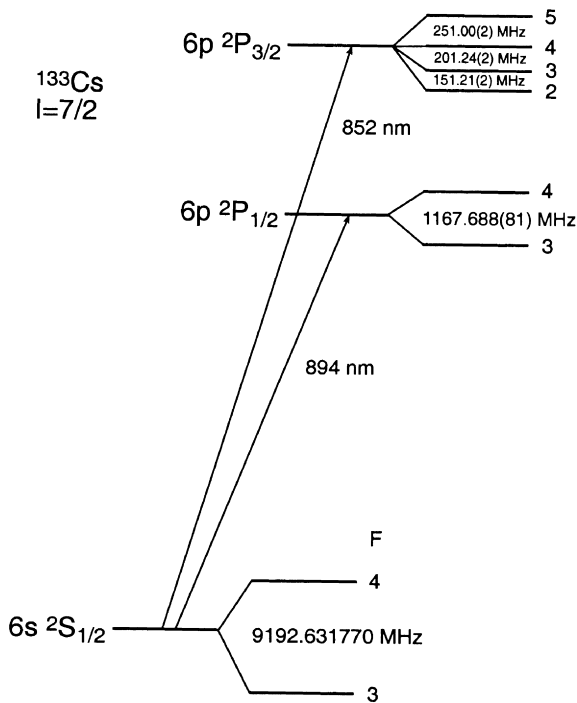


Fig. 1. Shown are the low lying electronic states of cesium with the rest frame transition wavelengths. The excited state hyperfine intervals are found in Refs. [14,15]. The ground state hyperfine interval is defined by international agreement. Longitudinal excitation of our fast atomic beam red shifts the resonances by about $10.6\ \text{cm}^{-1}$.

MHz of homogeneous broadening. Therefore a spectral bandwidth narrower than that of a free-running diode laser is not necessary. In a fast atomic beam, the acceleration process compresses the atomic velocities in the longitudinal direction. Therefore with colinear excitation of the fast beam, the excited state hyperfine structure is resolved, and the observed resonance widths depend most strongly upon the laser linewidth and the natural lifetime of the excited atomic state. Fig. 2 shows typical laser frequency scans of the fast atomic beam for both perpendicular and parallel excitation. Using the current controller and temperature stabilizer described in this paper, several of our accelerator runs were performed without active frequency locking since the laser required only minor adjustments between data runs at intervals of approximately 30 min. However, we also describe in this paper a simple and robust approach for absolute frequency locking of our lasers that will eliminate the need for these adjustments in future experiments. The stabilization technique employs radio-frequency (RF) modulation of the diode laser current in order to produce sidebands [4].

For excitation to the $6s\ ^2S_{1/2} \rightarrow 6p\ ^2P_{3/2}$ transition, we use a single-mode GaAs/GaAlAs diode laser, Model LT50A-03U from STC optical devices. This diode is selected for its wavelength near 852 nm and output power of about 50 mW at approximately 100 mA of forward current with a free-running bandwidth of less than 15 MHz. The injection current is supplied by a current controller of our own design described below. Rudimentary tuning is performed by adjusting and controlling the diode temperature which changes the effective semiconductor cavity length and index of refraction. Fine tuning and scanning of the laser is accomplished via control of the injection current. At constant temperature, these lasers tune continuously over a range of approximately 11 GHz by varying the injection current. For the $6s\ ^2S_{1/2} \rightarrow 6p\ ^2P_{1/2}$ transition, we use the commercially available Mitsubishi model ML 2701 lasers which provide 8 mW of output power at 894 nm with a forward current of 40 mA. The 40 MHz linewidth is slightly larger than that of the STC lasers. Although these two laser models have dif-

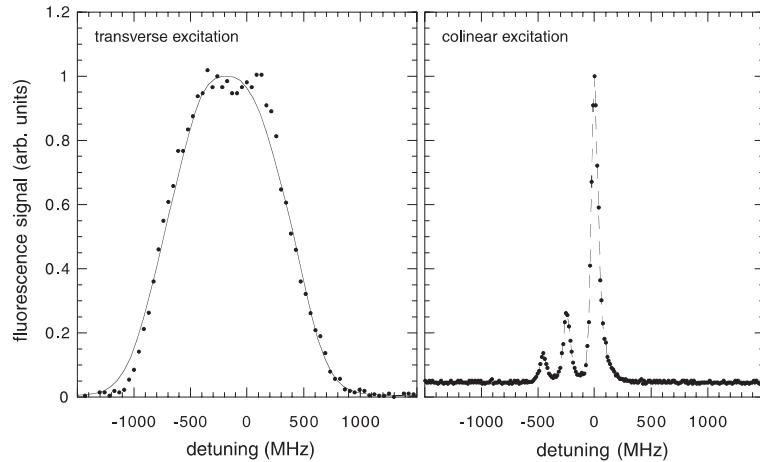


Fig. 2. Fast-beam fluorescence of the Cs $6p^2P_{3/2}$ excited state for both transverse and colinear laser excitation of the Cs $6s^2S_{1/2}$ $F = 4 \rightarrow 6p^2P_{3/2}$ $F' = 3, 4, 5$ transitions. Transversely excited, the spectral width is dominated by the transverse velocity distribution with an FWHM of 1.15 GHz. The solid line is the calculated lineshape. For colinear excitation, the spectral width is dominated by the laser linewidth, and the dashed line is simply a guide to the eye.

ferent electronic packages, they are both easily mounted in the same type of housing.

3. Temperature stabilization

We find that temperature can be controlled most precisely with the diode mounted in an air-tight housing. The temperature of the diode mount is sensed using a glass encapsulated bead thermistor, which is part of the temperature controller circuit that regulates the current to a Peltier thermoelectric cooler (TEC). The TEC pumps heat away from laser mount and into the housing which conducts it to the environment. To obtain the desired wavelength for some lasers, a small resistive heater is added to bring the laser mounting block near or above room temperature. In our circuit, the TEC always operates with a bias current in the cooling direction. We find that this approach simplifies the control circuit and eliminates the cross-over distortion that can occur in systems that are designed to both heat and cool with a single element. With the system we describe here, the diode temperature is regulated to within 7.5 mK peak to peak for hours at a time, which translates into excellent frequency stability.

3.1. Air-tight housing and laser mount

Our diode laser housing design is shown in Fig. 3. We use this particular design as our standard housing which can accommodate a variety of diode laser packages. The diode laser and collimating lens are mounted to an aluminum mounting block that is fixed to the surface of a TEC. Other materials with greater thermal conductivity, such as copper, may be used to construct the housing and/or mounting block. Aluminum is more easily machined, and we have not found additional thermal conduction to be necessary. The TEC removes heat from the mounting block and transfers it to the surrounding housing. The exterior of the housing remains near room temperature since the large external surface area of the housing removes heat by convection and by contact with the optical table. We have not found it necessary to use cooling fins on the exterior of the housing. Inside the housing, the laser-mounting block is held in place with four nylon screws that sandwich the TEC between the block and the base of the housing. The nylon screws prevent electrical and minimize heat conduction across the TEC. The laser package itself is mounted on a small aluminum cup that is fastened to the mounting block

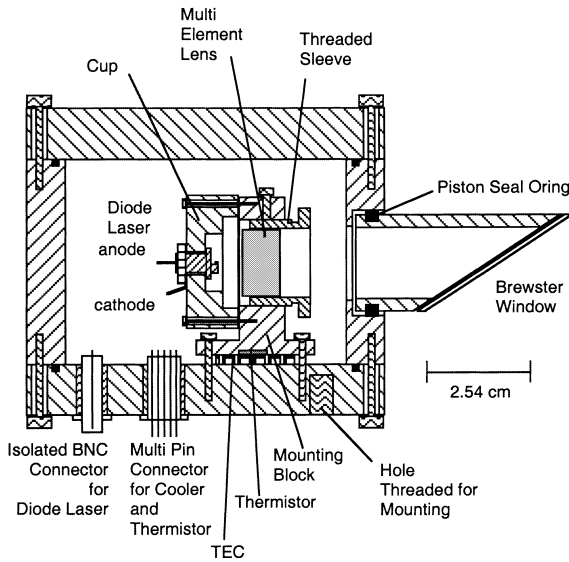


Fig. 3. The air-tight housing and laser mounting system are shown approximately to scale.

with metal screws. The cup makes good thermal contact to the mounting block and completely encloses the laser in a temperature-controlled environment with the electrical contacts passing through the bottom of the cup. The cup can be easily altered or replaced to accommodate different laser packages. The enlarged screw holes passing through the mounting cup allow for transverse position adjustments of the laser relative to the lens axis. We also design this hole pattern with 90° rotational symmetry so that the laser can be easily remounted for either vertical or horizontal polarization.

The diode mount also holds an adjustable 8.18 mm $f/0.55$ lens that collimates the rather divergent ($8^\circ \times 26^\circ$) laser output. The collimating lens is glued into a finely threaded sleeve that screws into the mounting block with 80 threads per inch. The threads allow the lens to be finely positioned relative to the laser, and a nylon screw locks the sleeve in place. When it can be controlled effectively, the small amount of passive feedback from the anti-reflection coated lens can be beneficial. Small adjustments to this feedback can be accomplished by changing the compression of the nylon screw that locks the lens in place. In this

mounting configuration, the laser itself is completely surrounded by temperature controlled surfaces including the lens. This approach has the added advantage that the optical path between the laser and the lens is also temperature stabilized minimizing drift in the small amount of optical feedback that comes from the lens surface.

Standard connectors for the laser current and temperature controller are mounted on the rigid aluminum base plate of the cylindrical housing. We also allow for a second multi-pin connector to power an optional Minco Model HK5207R12.5L12A Kapton-covered 12.5 Ω resistive heater that is typically attached to the side of the mounting block with thermal adhesive. Light exits the housing through a window glued to an aluminum tube with one end cut at Brewster's angle. The window is cut from a microscope slide into an elliptical shape to cover the output end of the tube. A piston-seal O-ring seals the tube into the wall of the housing. The piston seal O-ring allows the Brewster window to be rotated for different orientations of the linearly polarized laser light. The top and base flanges of the housing are also sealed with O-rings and held in place with screws. The cylindrical housing and circular flanges are designed for ease of machining and assembly. A solid metal spacer and base are attached to the outside of the bottom flange below the TEC so that heat can conduct to the large surface of the optical table.

3.2. Temperature controller

Temperature affects the laser wavelength through changes in the resonator length and index of refraction. The fundamental mode spacing of the plane parallel laser cavity is given by the expression

$$\nu_F = \frac{(c_0/n)}{2d}. \quad (1)$$

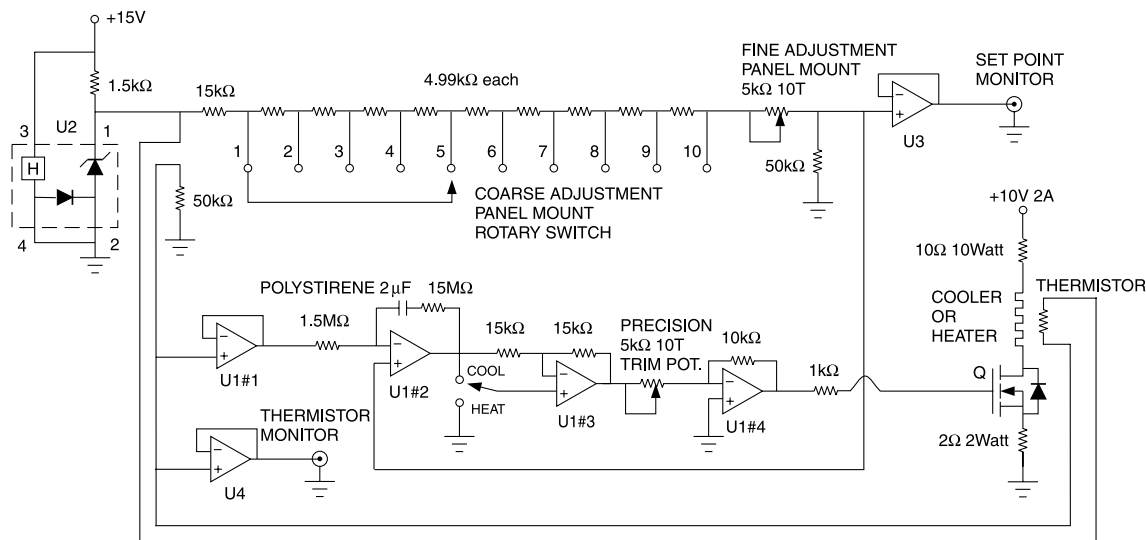
With an index of refraction of about $n = 3.5$ and a physical length of 532 μm [5], the laser cavity has a fundamental mode spacing of about $\nu_F = 80$ GHz. The laser operates at a wavelength that corresponds to an integer multiple of the fundamental mode spacing:

$$V_{out} = qV_F, \tag{2}$$

where $q = 1, 2, 3, 4, 5, \dots$. The STC lasers function near the cesium transition at 852.3 nm (vacuum wavelength) so the fundamental mode number is about $q = 4400$. The laser should tune continuously with temperature until a mode hop of approximately 80 GHz occurs. This allows one to tune the output easily over a wide range. However, to drive an atomic transition for long periods of time, these characteristics imply that the temperature be maintained to within a few mK for several hours. Therefore we have constructed the temperature control circuit shown in Fig. 4. An earlier version of this circuit, which was designed by one of us (C.E.T.), appears in Ref. [6].

We intend this temperature control circuit to operate in a fairly well controlled environment

(indoor room) where large and or rapid temperature changes are not expected. This allows us to keep the temperature servo simple by employing only integral feedback. The circuit is driven with a regulated ± 15 V power supply. The temperature of the diode laser mount is measured with a Fenwal 121-503JAJ-Q01 thermistor that has a nominal resistance of about 50 k Ω at room temperature. The thermistor resistance is inversely related to temperature as shown in Fig. 5. The thermistor is connected to the 6.95 V zener diode precision voltage reference, U2, in series with a 50 k Ω metal film resistor. The thermistor and the 50 k Ω fixed resistor act as a voltage divider. The voltage sensed between them, V_{temp} , is fed into the high impedance input of op-amp U1#1 that is wired as a voltage follower so only a negligible current is drawn from the divider. The measured voltage is given by



- NOTES:
 Regulated +15V and -15V are supplied to all operational amplifiers with filter capacitors to circuit ground.
 U1 is a TL074 quad operational amplifier package.
 U2 is an LM399 temperature stabilized 6.95V zener diode precision voltage reference.
 U3 and U4 are LF356 JFET input operational amplifiers.
 Q is a power MOSFET such as IRF 120, IRF 644, or GE/RCA C7840.
 The transistor and power resistors are heat sunk to the chassis off the printed circuit board.
 All resistors are 1% metal film, and all capacitors are low leakage such as polystyrene.
 The 5k Ω 10T trim pot is used to adjust the feedback gain until oscillations are eliminated.
 If oscillations persist the gain can be further reduced by changing the 15M Ω resistor on U1#2.
 The cooler or heater and thermistor are attached to the diode laser mount.
 A separate +10V power supply provides current for the cooler or heater.

Fig. 4. Temperature controller circuit.

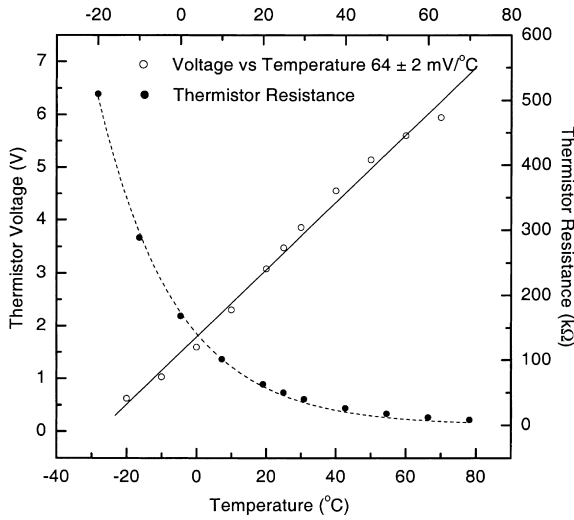


Fig. 5. Thermistor characteristics and voltage divider output as a function of temperature. With the chosen resistance values, there is an approximately linear relationship between voltage and temperature over the desired temperature range.

$$V_{temp} = \frac{50 \text{ k}\Omega}{50 \text{ k}\Omega + R_{therm}} \cdot 6.95 \text{ V.} \quad (3)$$

With this configuration, V_{temp} is roughly linear with temperature over the temperature range of interest as shown also in Fig. 5. A manually adjustable voltage divider is used to generate a set voltage, V_{set} , that is fed to the non-inverting high-impedance input of op-amp U1#2. V_{temp} is connected through a 1.5 MΩ resistor to the inverting input of U1#2. The feedback circuit on U1#2 integrates the difference between V_{set} and V_{temp} . The integrated error signal passes through op-amp U1#3 wired for unity gain with selectable sign then through op-amp stage U1#4 that has an adjustable gain. Finally, the error signal voltage appears at the gate of transistor Q and controls the current through the TEC. When we are using a TEC, the gain switch is in the COOL position. The same temperature controller can also be used with a heater in place of the TEC in which case the sign of the feedback is reversed by placing the switch in the HEAT position. In addition, there are two op-amps U3 and U4 wired as voltage followers that provide output signals for monitoring V_{set} and V_{temp} . When there is a voltage difference between V_{temp} and V_{set} and the gain switch is in the COOL

position, a current proportional to the integral of the difference flows through the TEC, and the laser is maintained at the temperature that corresponds to V_{set} . The gain of the integral feedback is adjusted to be slightly under damped so that large steps in V_{set} are removed after a couple of oscillations.

To test the temperature control circuit and airtight housing, we monitor V_{temp} and V_{set} over a period of 24 h with a Lab-View based data acquisition system using a National Instruments multi-function board. Samples are taken at a rate of 100 s⁻¹ with a 16 bit analog-to-digital converter. The samples are averaged over 1 min and converted to temperature using the calibration in Fig. 5. The room temperature is also monitored with a thermistor in air attached to a second temperature controller with no TEC. The results are plotted in Fig. 6. As a demonstration of the internal stability of the feedback loop, we compute the standard deviation in $T_{set} - T_{thermistor}$ over 1 h intervals and

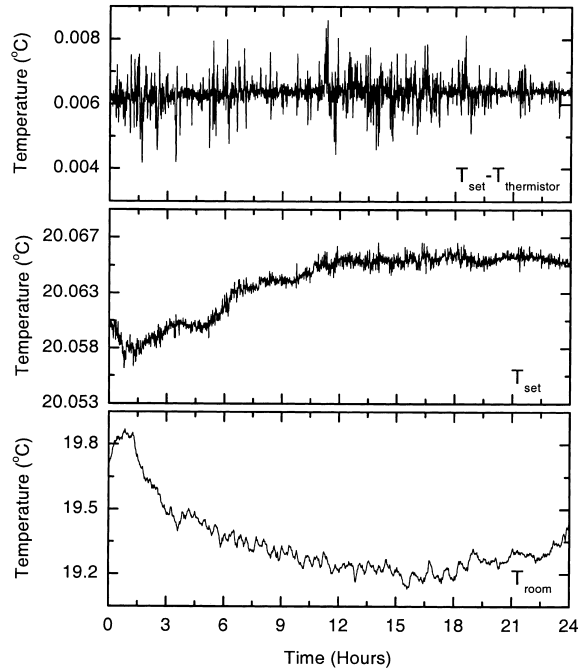


Fig. 6. Performance of the temperature controller versus time over a 24 h period. Samples are taken at a rate of 100 s⁻¹ and averaged to give one point per minute yielding 1440 points plotted on each graph. The standard deviation in $T_{set} - T_{thermistor}$ over 1 h is 4×10^{-5} K.

find 4×10^{-5} K. However, over the 24 h period T_{set} slowly drifts by a maximum of 7.5×10^{-3} K while $T_{\text{set}} - T_{\text{thermistor}}$ drifts by only 3×10^{-4} K. These slow drifts are correlated to the changes in room temperature with opposite sign. The room temperature drifts by -0.6 K over the same 24 h period. One might expect drifts in T_{set} that correlate to changes in room temperature since this part of the circuit is outside of the temperature controlled environment, and a drift in T_{set} will ultimately result in a change in laser temperature. The drift in $T_{\text{set}} - T_{\text{thermistor}}$ is less significant but can also be a result of temperature changes in the control circuit. Both drifts can be reduced by placing the entire circuit inside of the controlled environment of the air-tight housing. This modification is not practical for our diode laser application, but it could in principle be implemented for a system where temperature adjustment is not necessary and the size of the housing is not a constraint.

4. Current controller

The current controller is a stabilized DC source and provides two modulation channels for frequency tuning and control. Regulated ± 15 V power supplies drive the circuit shown in Fig. 7. We mount our lasers with their cathode at ground potential and current flows through the diode from the +15 V supply to ground. (For some lasers, we modify the circuit to place their anode at ground potential in which case current flows from ground through the laser to the negative supply. However, other changes are also necessary.) Transistor Q2 is part of a negative feedback loop that controls the current flow through the laser. The current also passes through a 50Ω Vishay four-wire current sensing resistor (VPH-4) in series with the laser. An instrumentation amplifier, U4, measures the voltage across the current sensing resistor with a gain of +1 and this signal is fed back to op-amp U2#1 of the TLO74 quad op-amp package U2 where it is added with a gain of -1 to a set voltage. The set voltage originates from a 6.95 V zener-diode voltage reference U1 in series with a current limiting resistor between 0 and -15 V. Two variable resistors provide for coarse and fine adjust-

ments of the negative set voltage. The voltage from the coarse adjustment resistor passes through the op-amp U2#2 with a gain of +2 then is summed with the voltages at op-amp U2#1 with a gain of -1 . The voltage from the fine adjustment resistor passes through U2#3 also with a gain of +2 then is summed with other voltages at op-amp U2#1 with a gain of $-1/100$. Two modulation inputs to the circuit pass through voltage followers (U3#1 and U3#4) and are also summed at U2#1 with gains of $-3/100$ each. The summed voltages are integrated by the op-amp U2#4 which drives transistor Q2 thus closing the feedback loop with high gain at DC. The output of the summing op-amp (U2#1) also passes through the op-amp U3#3 which provides a monitor of the error signal. The final op-amp in the circuit (U3#2) acts as a voltage follower to drive a voltmeter from the output from the instrumentation amplifier (U4). The actual laser current equals the voltmeter reading divided by 50Ω . The response of the current output to a modulation input has a 3 dB point at 4 kHz as shown in the Bode-type plot in Fig. 8. To test the noise characteristics under working conditions (100 mA forward current), we used a Tektronics 7000 Series oscilloscope with a variable bandwidth plug-in to measure the voltage noise across the 50Ω current-sensing resistor with the output shorted to ground. The results are given in Table 1.

5. Tuning characteristics

We studied the tuning characteristics of our lasers by controlling both the current and temperature. The model STC LT50A-03U single-longitudinal-mode diode lasers are specifically manufactured to operate at 852 nm at a temperature near 16°C . For a typical laser, we mapped out the wavelength as a function of laser temperature and injection current. The thermistor calibration for our temperature control circuit is shown in Fig. 5. The voltmeter output divided by 50Ω gives the current. A commercial Burleigh WA-10 wavelength meter with a resolution of 0.001 nm measures the wavelength. A 40 dB Isowave optical Faraday isolator between the laser and the wave-meter blocks the back-scattered reflections to

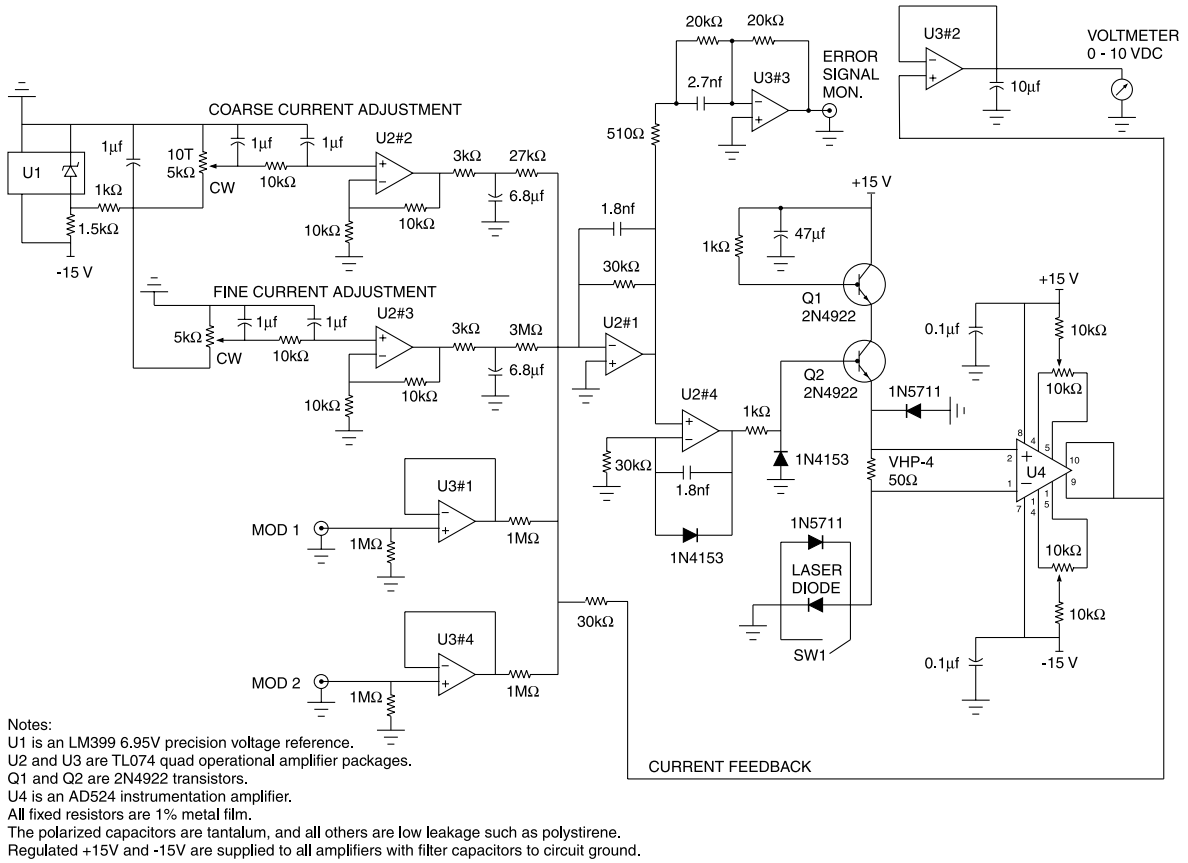


Fig. 7. Current controller circuit.

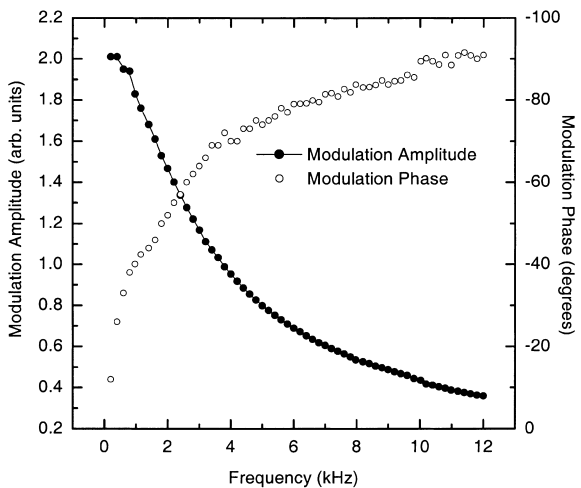


Fig. 8. Current controller modulation characteristics showing both amplitude and phase as a function of frequency.

Table 1
 Current controller noise measured across a 50 Ω load

Noise type	Voltage (peak to peak)	Bandwidth
60 Hz	0.2 mV	–
Broad band	100 μV	1 MHz
Broad band	10 μV	30 kHz

The noise at 60 Hz originates from the 120 V AC to ±15 V DC power supply. This noise can be eliminated by driving the current controller with batteries.

eliminate optical feedback. The results are displayed in Fig. 9. The gray scaled contour plot shows several wavelength regions where the laser tunes smoothly in a single mode without mode hopping for a wide range of currents and temperatures. The darker regions correspond to

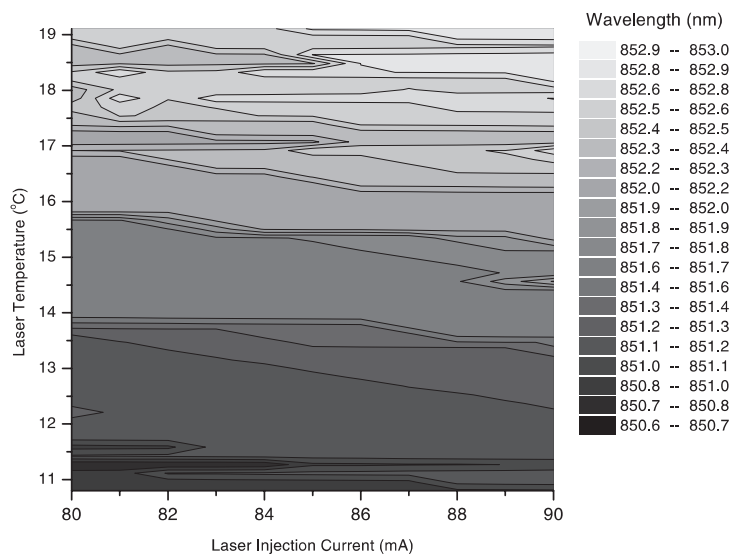


Fig. 9. Laser wavelength dependance on temperature and current.

shorter wavelengths and the lighter regions to longer wavelengths. Within a region of uniform grayness at fixed temperature, the laser tunes continuously at a rate of 2.7 GHz mA^{-1} over frequency intervals of as much as 11 GHz before a mode hop occurs. At fixed current, the laser tunes smoothly at a rate of 19.6 GHz K^{-1} . The contours are closely spaced near regions where a mode hop occurs. However, each mode hope corresponds to an abrupt change in wavelength of approximately 78 GHz which we estimate to be the laser's longitudinal mode spacing. During normal operation, we select the temperature and current of the laser to obtain the desired wavelength in a region that is far from mode hops.

6. Current feedback using sidebands

An important requirement in precision spectroscopy experiments is that the laser frequency remains fixed over a long period of time. Due to its intrinsic characteristics, the output of a diode laser may change in frequency in spite of our best efforts to control both the temperature and injection current. This residual drift in our case is due to a combination of temperature variations in the

control electronics and laser aging. To eliminate such drifts, a laser can be frequency locked to a stable reference (optical cavity, atomic transition, or molecular transition). Feedback from the reference can be provided optically and/or electronically [7,8]. In our case, the stable references are the various hyperfine components of the ^{133}Cs $6s^2\text{S}_{1/2} \rightarrow 6p^2\text{P}_{1/2}$ and $6p^2\text{P}_{3/2}$ resonance transitions. One widely used technique [9] locks the laser to a Doppler-free saturated absorption [10,11] signal in a thermal cell using laser current modulation at a rate of near 1 kHz with a modulation depth of about 8 MHz and a lock-in amplifier. A typical saturated absorption scan recorded with our own optical setup is shown in Fig. 10. This technique has some drawbacks in our fast-beam application. The broad linewidth of the free-running diode laser (15 to 40 MHz depending on the laser type) requires a large depth of the modulation thus adding to the frequency noise. In testing this technique, we increased the modulation frequency to 30 kHz in order to reduce the modulation depth (2–3 MHz), however the reduction in frequency noise was not satisfactory. The error signal is also sensitive to scattered and room light and mechanical vibrations in the optical system. In addition, the back-propagating saturation beam can

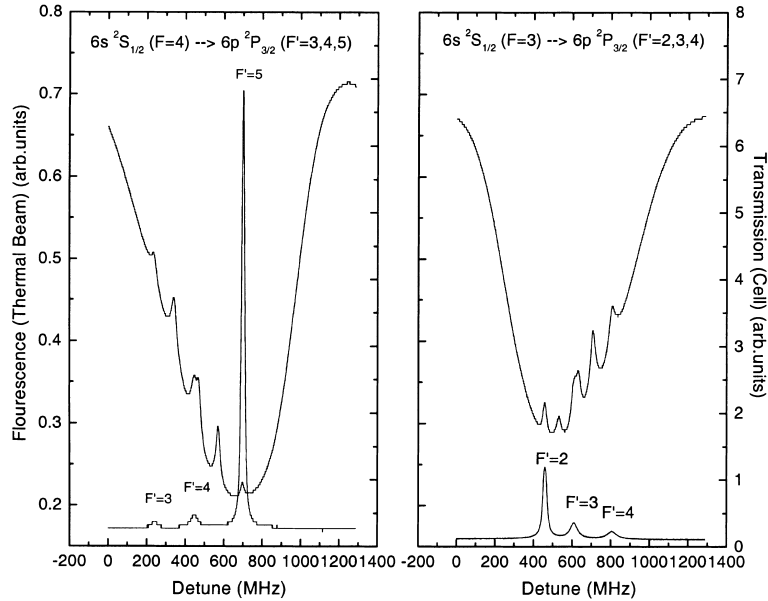


Fig. 10. ^{133}Cs cell transmission showing the effects of saturated absorption on the $6s^2S_{1/2} \rightarrow 6p^2P_{3/2}$ transition. The fluorescence from a collimated thermal Cs beam shows the resolved hyperfine structure and provides a calibration for the frequency scale.

cause optical feedback to which diode lasers are extremely sensitive. Another disadvantage is that the width of the error signal is only several MHz localized near one of the saturation peaks. Thus the laser frequency cannot be tuned much by adding a DC offset to the error signal. A wide tuning range is important in our fast-beam experiments because the transitions can be significantly Doppler-shifted when the laser and the atomic velocities are not exactly perpendicular. For example, in our fast-beam experiment, the neutral Cs beam is formed by charge exchange from Cs^+ ions accelerated through a 50 keV potential. In this case, the atoms are moving at about $2.7 \times 10^7 \text{ cm s}^{-1}$, resulting in Doppler detunings of 35 MHz mrad^{-1} . Our apparatus does not allow much freedom to adjust the angle between the laser and the atomic beam in order to compensate for a large frequency offset. To avoid some of these problems, we propose using a sideband locking technique similar to that of Drever [4] but use an Cs absorption cell [12] instead of a resonant cavity.

Our frequency locking scheme is shown in Fig. 11. The diode laser current is modulated at 70

MHz through an RF-bias T mounted directly between the diode laser and the current controller. The sidebands lie outside the laser linewidth. An RF power of -26 dBm transfers 8% of the optical carrier into the sidebands. The laser output with sidebands is sent through a Cs absorption cell. The transmitted light is detected with a fast photodiode (New-Focus Model 1621) and the signal is sent to a double balanced mixer (Minicircuits Model ZFM-3) for demodulation. The room-temperature Doppler-broadened Cs transition combined with demodulation of the RF signal produces a broad error signal with a high signal-to-noise ratio. An example of the error signal produced with a 5 cm long Cs cell is shown in Fig. 12. Simultaneously, the fluorescence from a collimated atomic beam is recorded as a frequency calibration. The laser can be locked at any point within an approximately 200 MHz wide frequency interval by adding a DC offset to the error signal. By optimizing the error signal amplitude, this technique also reduces the laser linewidth to approximately 10 MHz. The linewidth can be further reduced by employing a faster feedback circuit and optimizing its phase [13]. With this scheme, the laser stays locked for

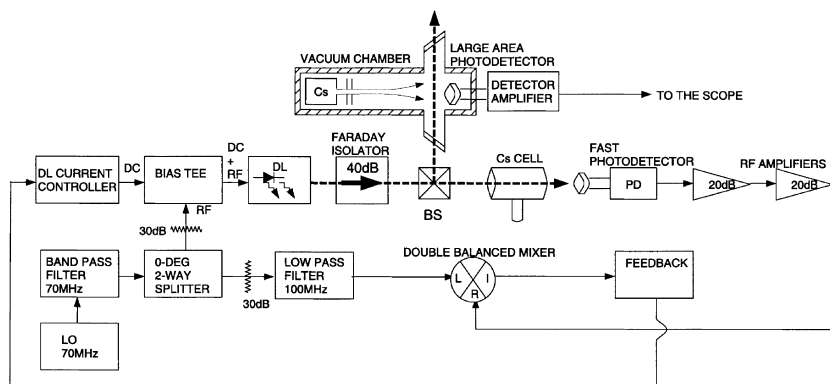


Fig. 11. Experimental setup for laser frequency locking.

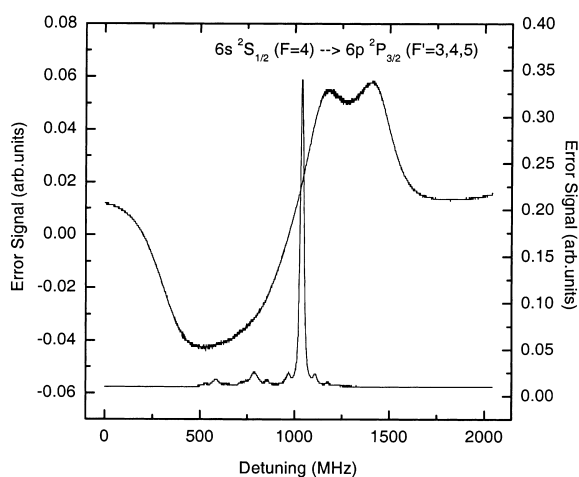


Fig. 12. The output of the double balanced mixer produces a feedback error signal for stabilizing the laser frequency. By adding an offset, the laser can be locked to any point along the central slope of the error signal. Fluorescence from the collimated thermal Cs beam provides a frequency scale and shows the presence of RF sidebands on the laser output.

hours, requiring minimal manual adjustment. The system is very insensitive to mechanical vibrations because the error signal depends little on the particulars of the optical alignment. In addition, the error signal is insensitive to low frequency changes in room or scattered light levels. At present, factors limiting our capability to reduce the laser linewidth include the magnitude of the error signal, the bandwidth of the electronic feedback circuit (unity gain at 100 kHz), and the bandwidth of

the laser current controller (3 dB point at approximately 4 kHz, see Fig. 8).

7. Conclusions

This paper describes the diode laser system that we have successfully developed for our fast-beam laser experiments. The system comprises a low noise DC source, an air-tight housing, and a temperature stabilization circuit that maintains the temperature of the diode laser to within several mK. Each element of the system is described in sufficient detail to allow other researchers to use this work to build their own system. We also discuss a simple robust frequency locking scheme that can be easily added to a free running diode laser system similar to the one we describe here.

Acknowledgements

Financial support for this work was provided by the Division of Chemical Sciences, Office of Basic Energy Sciences, Office of Energy Research at the US Department of Energy under contract number DE-FG02-95ER14579. One of us (S.T.R.) would also like to acknowledge support by the US Department of Energy, through the Division of Materials Sciences, grant number DE-FG02-88ER45373.

References

- [1] R.J. Rafac, C.E. Tanner, A.E. Livingston, H.G. Berry, *Phys. Rev. A* 60 (5) (1999) 3648.
- [2] D. DiBerardino, R.J. Rafac, D.M. Glantz, C.E. Tanner, *Opt. Commun.* 143 (1997) 118.
- [3] C.E. Wieman, L. Hollberg, *Rev. Sci. Instrum.* 62 (1) (1991) 1.
- [4] R.W. Drever, J.L. Hall, F.V. Kowalski, J. Hough, G.M. Ford, A.J. Munley, H. Ward, *Appl. Phys. B* 31 (1983) 97.
- [5] S.R. Kisting, P.W. Bohn, E. Andideh, I. Adesida, B.T. Cunningham, *Appl. Phys. Lett.* 57 (13) (1990) 1328.
- [6] K.B. MacAdam, A. Steinbach, C.E. Wieman, *J. Phys.* 60 (1992) 1098.
- [7] B. Dahmani, L. Hollberg, R. Drullinger, *Opt. Lett.* 12 (1987) 876.
- [8] M. Ohtsu, *Opt. Quant. Electron.* 20 (1988) 283.
- [9] H. Hori, Y. Kitayama, M. Kitano, T. Yabuzaki, T. Ogawa, *IEEE QE-19* (1983) 169.
- [10] T.W. Hänsch, M.H. Nayfeh, S.A. Lee, S.M. Curry, I.S. Shahin, *Phys. Rev. Lett.* 32 (1974) 1336.
- [11] H. Berhardt, E. Matthias, F. Schneider, A. Timmermann, *Z. Phys. A* 3288 (1978) 327.
- [12] S. Kunze, S. Wolf, G. Rempe, *Opt. Commun.* 128 (1996) 269.
- [13] L. Ricci, M. Weidemüller, T. Esslinger, A. Hemmerich, C. Zimmermann, V. Vuletic, W. König, T.W. Hänsch, *Opt. Commun.* 117 (1995) 541.
- [14] C.E. Tanner, C. Wieman, *Phys. Rev. A* 38 (3) (1988) 1616.
- [15] T. Udem, J. Reichert, R. Holzwarth, T.W. Hänsch, *Phys. Rev. Lett.* 82 (1999) 3568.